*Journal of Sound and Vibration* (2000) **229**(2), 311–327
*Article No.* jsvi.1999.2485, available online at http://www.idealibrary.com on IDEAL®

# FREE VIBRATION OF CLAMPED ORTHOTROPIC SANDWICH PANEL

T. S. LOK AND Q. H. CHENG
*Nanyang Technological University, School of Civil and Structural Engineering, Nanyang Avenue, Singapore* 639798

(*Received* 19 *March* 1999, *and in final form* 14 *June* 1999)

Sandwich panels are thin-walled structures fabricated from two flat sheets, separated by and attached to a core. An analytical solution for the dynamic response of such structures is not available but equivalency in the form of a homogenous orthotropic thick plate can be formulated. This paper considers a truss-core sandwich panel that is similar to conventional sandwich systems, but eliminates many of the attendant problems associated with fabrication of conventional forms. The dynamic response of the truss-core sandwich panel is then formulated as a homogeneous orthotropic thick plate. Closed-form solution for a clamped plate is derived. Closed-form solutions are compared with both 2- and 3-D finite element results. Excellent agreement of response is obtained.


## 1. INTRODUCTION

Sandwich panels have been successfully used for many years in the aviation and aerospace industries, as well as in marine, and mechanical and civil engineering applications. This is due to the attendant high stiffness and high strength to weight ratios of sandwich systems. An example is the traditional honeycomb-core sandwich panel. Detailed treatment of the behavior of honeycombed and other types of sandwich panels can be found in monographs by Plantema [1] and Allen [2]. Several types of conventional thin-walled sandwich panels, which are distinguishably different from the honeycombed sandwich form, have also been investigated [3–8]. These structures are characterized by a common feature of two flat facing sheets, but the core takes many generic forms; continuous corrugated sheet or a number of discrete but aligned longitudinal top-hat, zed or channel sections (see Figures 1(a)–(d)). The core and facing plates are joined by spot-welds, rivets or self-tapping screws.

Figure 1(e) shows a type of sandwich panel construction that the authors have recently investigated. This truss-core sandwich panel is made of a number of symmetrical truss-core panel units in which the core webs are built into the facing plates. The unit may be fabricated from an extrusion process, and made from aluminum or fiber reinforced plastic. Units are then welded/interlocked along the edges of the facing plates to form a wide sandwich panel. This construction

0022-460X/00/020311 + 17 $35.00/0 

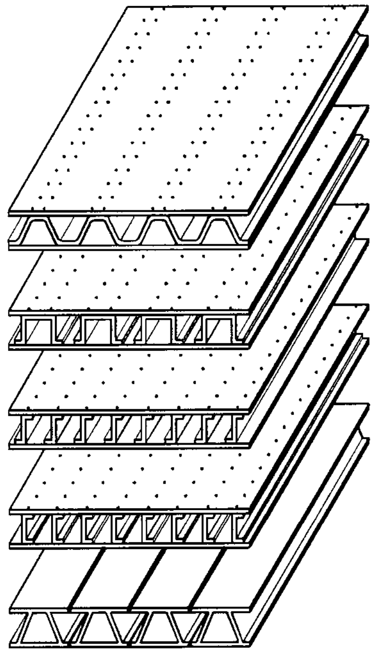


Figure 1. Sandwich panel with (a) continuous corrugated-core, (b) top-hat core, (c) zed-core, (d) channel-core and (e) truss-core.

form has many advantages over those shown in Figures 1(a)–(d); some of which are

- The elimination of discrete connections and all its attendant problems. This is crucial for structures or vessels designed to maintain pressure and water-tightness between the outer and inner environments.
- Better material utilization and ease of manufacturing since only one extrusion process is needed. Transportation, handling and construction cost would be reduced since no large flexible thin sheets are involved.
- Promotion of designer flair to create curved shapes that linear flat conventional sandwich panels are unable to provide.

Thin-walled sandwich panels are relatively complex 3-D systems. Since no analytical solution exists, the 3-D finite element method is commonly employed to analyze the structure. This is a tedious and uneconomical task if the user is unfamiliar with hardware and software systems. However, 3-D FE analysis may be avoided by transforming the panel into an equivalent homogeneous orthotropic thick plate continuum and then analyzing the resulting orthotropic thick plate by a closed-form solution. To facilitate the transformation, seven equivalent elastic constants are required, five of which ($D_x$, $D_y$, $D_{xy}$, $D_{Qx}$ and $D_{Qy}$) are shown in Figure 2. The other two are the bending Poisson ratios, $\nu_x$ and $\nu_y$. Elastic constants of sandwich panels with continuous corrugation core, channelized cores and

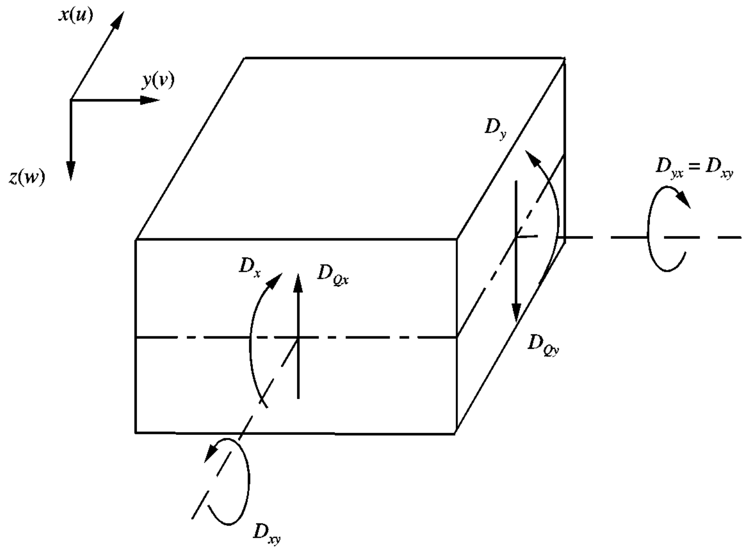


Figure 2. Stiffness constants of thick plate continuum.

truss-core have been obtained by Libove and Hubka [3], Fung *et al.* [7, 8] and by the authors [9] respectively. 2-D bending analysis has been conducted using closed-form solution [2, 9] and thick-plate finite element [10]. Recently, the response of simply supported orthotropic sandwich panels was investigated [11] from which natural frequencies and forced response were obtained by utilizing double series functions as mode shapes.

## 2. DYNAMIC ANALYSIS OF CLAMPED ORTHOTROPIC PLATE

For orthotropic plates with clamped boundary conditions, the problem of flexural vibration is relatively more complicated but this has been investigated extensively. While an exact solution is not available, approximate solutions are abundant for orthotropic plates. Leissa [12] presented an excellent summary of earlier studies on the topic. Sakata and Hosokawa [13] proposed a double trigonometric series solution for forced and free vibration analysis while the method of superposition for free vibration was exploited by Gorman [14]. The latter technique was extended to include forced vibration by Li [15]. The Kantorovich method was introduced to study free vibration response of clamped orthotropic plates [16, 17]. However, these reports are limited to thin plates. For thick plates, the influence of transverse shear on the vibration response cannot be ignored. To predict the dynamic response of thick plates including transverse shear, Ramkumar *et al.* [18] utilized the Lagrangian multiplier technique. One of the drawbacks of their solution is that when the number of Lagrangian multiplier is not equal to the number of vibration modes to be computed, the mode shape functions may not satisfy fully the boundary conditions, thus resulting in an accumulation of numerical errors. Another disadvantage of this technique is that the natural frequencies of a simply supported plate have to be computed before the algorithm operation can be conducted for the clamped plate.

In this paper, the dynamic behavior of clamped orthotropic sandwich panels is investigated by utilizing the derived equivalent elastic constants. This synergy allows a closed-form solution to be developed to calculate the natural frequencies of an equivalent rectangular orthotropic thick plate continuum. The Rayleigh–Ritz method [19] is utilized for this purpose. Admissible functions are determined from the mode shapes of corresponding clamped thick beams, including the effect of transverse shear deformation and moment of inertia. These functions satisfy the boundary conditions of the clamped plate. Comparison of results of natural frequencies shows the accuracy of the solution derived from the present approach. The solution is shown to be better than that calculated from the Lagrangian multiplier technique [18]. Following this verification, a truss-core sandwich panel is investigated by the present closed-form solution and by finite element analysis. The first 10 natural frequencies of free vibration for the clamped orthotropic thick plate are computed. Excellent agreement is observed between closed-form solution and finite element results.

## 3. ELASTIC CONSTANTS OF ORTHOTROPIC PLATE AND SANDWICH PANEL

The general small-deflection theory developed by Libove and Batdorf [20] was adopted to describe the flexural behavior of an orthotropic plate. Seven elastic constants represent the properties of the thick plate. These have been described earlier, in which $D_x$ and $D_y$ represent bending stiffnesses, $\nu_x$ and $\nu_y$ are the bending Poisson ratios, $D_{xy}$ is the twisting stiffness, and $D_{Qx}$ and $D_{Qy}$ are the transverse shear stiffnesses (see Figure 2). For a conventional orthotropic plate of thickness $h$, the stiffnesses are given as

$$D_x = \frac{E_x h^3}{12}, \qquad D_y = \frac{E_y h^3}{12}, \qquad D_{xy} = \frac{G_{xy} h^3}{6}, \tag{1a}$$

$$D_{Qx} = k^2 G_{xz} h, \qquad D_{Qy} = k^2 G_{yz} h, \tag{1b}$$

where $E_x$ and $E_y$ are the elastic moduli and $G_{xy}$, $G_{xz}$ and $G_{yz}$ are the shear moduli. $k^2$ is the transverse shear correction factor and is usually taken as $\pi^2/12$ or an approximate figure [18].

Equivalent elastic constants for the truss-core panel have been derived by the authors [9]. To express these elastic constants, consider the truss-core sandwich unit shown in Figure 3. The unit is symmetrical with respect to a vertical plane. The upper and lower facing plates have the same thickness ($t_f$) while the core's thickness ($t_c$) may differ from the facing plates. Independent geometric dimensions are described by $p$, $d$, $t_f$ and $t_c$. Three dimensions, $f$, $l$ and $\theta$ are dependent on each other. Three other dimensions, $d_c$, $b_c$ and $f_0$ are obtained from geometric properties. Material properties are elastic modulus $E$, shear modulus $G$ and the Poisson ratio $\nu$.

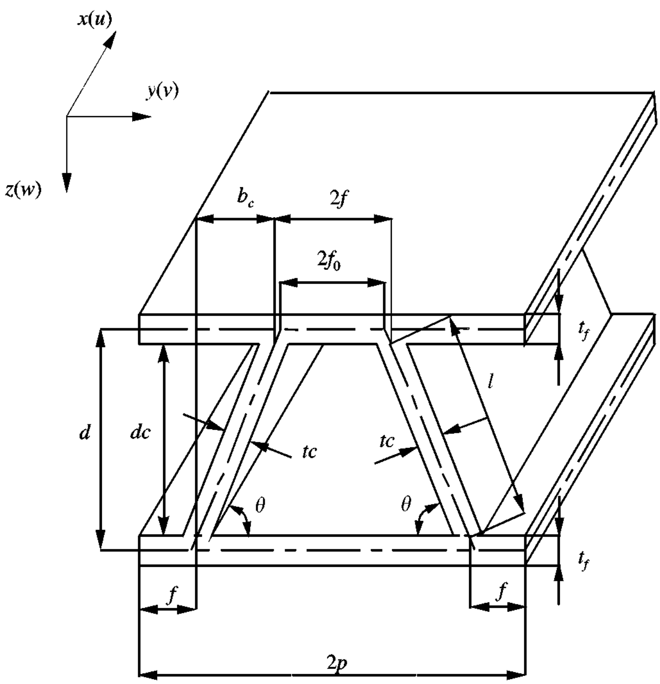


Figure 3. Dimensions of truss-core sandwich panel unit.

Elastic constants of the truss-core unit derived by the authors are

$$D_x = E(I_c + I_f), \qquad D_y = \frac{EI_f}{1 - \nu^2 I_c/(I_c + I_f),} \tag{2a}$$

$$D_{xy} = GI_f, \qquad \nu_x = \nu, \qquad \nu_y = \nu\frac{D_y}{D_x}, \tag{2b}$$

$$D_{Qx} = Gt_c\frac{\mathrm{d}^2 t_f/plt_c + \frac{1}{6}(\mathrm{d}_c/p)^2}{t_f/t_c + ld_c/3pd}, \qquad D_{Qy} = \frac{1}{(\delta_y^C + \delta_y^F)/d + \delta_z^C/p}, \tag{2c}$$

where $\delta_y^C$, $\delta_z^C$ and $\delta_y^F$ are deflection parameters described in reference [9]; $I_c$ and $I_f$ are the moments of inertia per unit width of the truss-core cross-section in the $yz$-plane defined as

$$I_c = \frac{lt_c d_c^2}{12p}, \qquad I_f = \frac{t_f d^2}{2}. \tag{3}$$

## 4. NATURAL FREQUENCY AND MODE SHAPE

### 4.1. GOVERNING DIFFERENTIAL EQUATIONS

Libove's small-deflection theory is extended for vibration analysis by including mass and moment of inertia of the plate. The governing differential equations may be written as

$$D_{Qx}\left(\frac{\partial^2 w}{\partial x^2}-\frac{\partial \theta_x}{\partial x}\right)+D_{Qy}\left(\frac{\partial^2 w}{\partial y^2}-\frac{\partial \theta_y}{\partial y}\right)+q=\rho h\frac{\partial^2 w}{\partial t^2}, \tag{4a}$$

$$D_{Qx}\left(\frac{\partial w}{\partial x}-\theta_x\right)+\frac{D_{xy}}{2}\left(\frac{\partial^2\theta_x}{\partial y^2}+\frac{\partial^2\theta_y}{\partial x\,\partial y}\right)+\frac{D_x}{g}\left(\frac{\partial^2\theta_x}{\partial x^2}+v_y\frac{\partial^2\theta_y}{\partial x\,\partial y}\right)=J_x\frac{\partial^2\theta_x}{\partial t^2}, \tag{4b}$$

$$D_{Qy}\left(\frac{\partial w}{\partial y}-\theta_y\right)+\frac{D_{xy}}{2}\left(\frac{\partial^2\theta_y}{\partial x^2}+\frac{\partial^2\theta_x}{\partial x\,\partial y}\right)+\frac{D_y}{g}\left(\frac{\partial^2\theta_y}{\partial y^2}+v_x\frac{\partial^2\theta_x}{\partial x\,\partial y}\right)=J_y\frac{\partial^2\theta_y}{\partial t^2}, \tag{4c}$$

where $g = 1 - v_x v_y$, $q$ represents lateral loading acting on the surface of the plate, $w$ is the displacement at a point in the plate in the $z$ direction, $\theta_x$ and $\theta_y$ are rotations of the normal of the plate with respect to the $y$- and $x$-axis, respectively, $\rho$ is the material density of the plate, $J_x$ and $J_y$ are moments of inertia per unit area of the plate in the $x$ and $y$ directions respectively; and $t$ denotes time. It may be observed that equation (4) is a first order shear deformation theory. Consequently, the transverse shear strain is constant across the thickness of the plate.

Consider a rectangular orthotropic thick plate of length $a$, width $b$ and thickness $h$ in the $x$, $y$ and $z$ directions respectively. The clamped boundary conditions are

$$x = 0,\quad a: w = 0,\quad \theta_x = \frac{\partial w}{\partial x} = 0, \tag{5a}$$

$$y = 0,\quad b: w = 0,\quad \theta_y = \frac{\partial w}{\partial y} = 0. \tag{5b}$$

For the plate in harmonic motion, the deflection and rotations are assumed to take the form

$$w = W(x, y)\sin(\omega t + \varphi_0) = \left(\sum_{m=1}^{\infty}\sum_{n=1}^{\infty} a_{mn} W_{xm}(x) W_{yn}(y)\right)\sin(\omega t + \varphi_0), \tag{6a}$$

$$\theta_x = \Phi_x(x, y)\sin(\omega t + \varphi_0) = \left(\sum_{m=1}^{\infty}\sum_{n=1}^{\infty} b_{mn} \Psi_{xm}(x) W_{yn}(y)\right)\sin(\omega t + \varphi_0), \tag{6b}$$

$$\theta_y = \Phi_y(x, y)\sin(\omega t + \varphi_0) = \left(\sum_{m=1}^{\infty}\sum_{n=1}^{\infty} c_{mn} W_{xm}(x) \Psi_{yn}(y)\right)\sin(\omega t + \varphi_0), \tag{6c}$$

where $a_{mn}$, $b_{mn}$ and $c_{mn}$ are mode shape coefficients; the mode shape functions $W_{xm}$, $\Psi_{xm}$, $W_{yn}$ and $\Psi_{yn}$ are derived from the eigenvalue problem of a beam clamped at $x = 0$, $a$ and $y = 0$, $b$ respectively.

### 4.2. BEAM FUNCTIONS

The differential equation (4) and boundary condition (5) may be simplified for free vibration of a clamped beam as

$$D_{Qx}\left(\frac{\partial^2 w}{\partial x^2}-\frac{\partial \theta_x}{\partial x}\right)=\rho h\frac{\partial^2 w}{\partial t^2}, \tag{7a}$$

$$D_{Qx}\left(\frac{\partial w}{\partial x}-\theta_x\right)+\frac{D_x}{g}\left(\frac{\partial^2 \theta_x}{\partial x^2}\right)=J_x\frac{\partial^2 \theta_x}{\partial t^2}, \tag{7b}$$

$$x=0,\quad a: w=0,\quad \theta_x=\frac{\partial w}{\partial x}=0. \tag{8}$$

When the beam is vibrating in its $m$th order natural frequency $\omega_m$, the deflection and rotation can be expressed as

$$w(x,t)=W_{xm}(x)\sin(\omega_m t+\varphi_0), \tag{9a}$$

$$\theta_x(x,t)=\Psi_{xm}(x)\sin(\omega_m t+\varphi_0). \tag{9b}$$

Substituting equation (9) into equation (7) and rearranging give

$$\frac{\partial^4 W_{xm}}{\partial x^4}+\omega_m^2\left(\frac{\rho h}{D_{Qx}}+\frac{gJ_x}{D_x}\right)\frac{\partial^2 W_{xm}}{\partial x^2}+\omega_m^4\frac{\rho h}{D_{Qx}}\frac{gJ_x}{D_x}W_{xm}-\omega_m^2\frac{g\rho h}{D_x}W_{xm}=0, \tag{10a}$$

$$\left(\frac{gD_{Qx}}{D_x}-\frac{\omega_m^2 gJ_x}{D_x}\right)\Psi_{xm}=\frac{\partial^3 W_{xm}}{\partial x^3}+\frac{gD_{Qx}}{D_x}\frac{\partial W_{xm}}{\partial x}+\omega_m^2\frac{\rho h}{D_{Qx}}\frac{\partial W_{xm}}{\partial x}. \tag{10b}$$

The solution of equation (10) takes the form

$$W_{xm}=A_1\cosh(s_1x)+A_2\sinh(s_1x)+A_3\cos(s_0x)+A_4\sin(s_0x), \tag{11a}$$

$$\Psi_{xm}=B_1\cosh(s_1x)+B_2\sinh(s_1x)+B_3\cos(s_0x)+B_4\sin(s_0x), \tag{11b}$$

where $s_1$ and $s_0$ are obtained from

$$\frac{s_1}{s_0}=\frac{\omega_m}{\sqrt{2}}\sqrt{\mp\left(\frac{\rho h}{D_{Qx}}+\frac{gJ_x}{D_x}\right)+\sqrt{\left(\frac{\rho h}{D_{Qx}}-\frac{gJ_x}{D_x}\right)^2+\frac{4g\rho h}{\omega_m^2 D_x}}}. \tag{12}$$

The frequency $\omega_m$ and the coefficients $A_1-A_4$ and $B_1-B_4$ in equation (11) are determined from the clamped boundary conditions given in equation (8). $A_1$ is set to unit value and all the unknown coefficients are normalized to $A_1$.

The functions $W_{yn}$ and $\psi_{yn}$ take a form similar to $W_{xm}$ and $\psi_{xm}$ but with $y$ replacing $x$, $b$ replacing $a$ in the boundary conditions, etc. Substituting $W_{xm}$, $\psi_{xm}$,

$W_{yn}$ and $\psi_{yn}$ into equation (6), it can be shown that expressions of displacement and rotations given in equation (6) satisfy the boundary conditions in equation (5).

### 4.3. NATURAL FREQUENCIES OF ORTHOTROPIC PLATE

The total strain energy $U$ and kinetic energy $T$ of the plate may be written, respectively, as

$$U = \frac{1}{2}\iint_{\Omega}\left\{\frac{D_x}{g}\left(\frac{\partial\theta_x}{\partial x}\right)^2 + \frac{D_x\nu_y + D_y\nu_x}{g}\frac{\partial\theta_x}{\partial x}\frac{\partial\theta_y}{\partial y} + \frac{D_y}{g}\left(\frac{\partial\theta_y}{\partial y}\right)^2 + \frac{D_{xy}}{2}\left(\frac{\partial\theta_y}{\partial x} + \frac{\partial\theta_x}{\partial y}\right)^2 + D_{Qx}\left(\frac{\partial w}{\partial x} - \theta_x\right)^2 + D_{Qy}\left(\frac{\partial w}{\partial y} - \theta_y\right)^2\right\}\mathrm{d}x\,\mathrm{d}y, \tag{13a}$$

$$T = \frac{\rho h}{2}\iint_{\Omega}\left(\frac{\partial w}{\partial t}\right)^2\mathrm{d}x\,\mathrm{d}y + \frac{1}{2}\iint_{\Omega}\left[J_x\left(\frac{\partial\theta_x}{\partial t}\right)^2 + J_y\left(\frac{\partial\theta_y}{\partial t}\right)^2\right]\mathrm{d}x\,\mathrm{d}y, \tag{13b}$$

where the integration is over the domain $\Omega$ of the plate in the $x$–$y$ plane.

According to Hamilton's principle for free vibration

$$\delta\int_{t_1}^{t_2}(T - U)\,\mathrm{d}t = 0, \tag{14}$$

where $\delta$ is a variational operator.

The infinite series in equation (6) may be truncated without significant loss of accuracy by summing up from $m = n = 1$ up to $m = M$ and $n = N$. Substituting the differentials of equation (6) into equation (13) and then integrating over the domain $\Omega$, $T$ and $U$ are obtained as functions of time ($t$). Thereafter, by substituting $T$ and $U$ into equation (14), a set of simultaneous equations is obtained:

$$[K]\{a\} = 0, \tag{15}$$

where $\{a\}$ is a vector of unknowns and $[K]$ is a square matrix, expressed as

$$\{a\} = [a_{11}\ \ b_{11}\ \ c_{11}\ \ a_{12}\ \ b_{12}\ \ c_{12}\ \ \cdots\ \ a_{MN}\ \ b_{MN}\ \ c_{MN}]^{\mathrm{T}}, \tag{16}$$

$$[K] = \begin{bmatrix} [K_{11}^{11}] & [K_{12}^{11}] & \cdots \\ [K_{11}^{12}] & [K_{12}^{12}] & \cdots \\ \cdots & [K_{ij}^{mn}] & \cdots \\ \cdots & \cdots & [K_{MN}^{MN}] \end{bmatrix}. \tag{17}$$

The elements of the sub-matrices of $[K]$ are obtained by integrating the products of beam functions or their derivatives, and may be expressed as

$$[K_{ij}^{mn}]_{11} = D_{Qx} X_{\mathrm{d}W} Y_W + D_{Qy} X_W Y_{\mathrm{d}W} - \omega^2 \rho h X_W Y_W, \tag{18a}$$

$$[K_{ij}^{mn}]_{12} = -D_{Qx} X_{\mathrm{d}W\Psi} Y_W, \tag{18b}$$

$$[K_{ij}^{mn}]_{13} = -D_{Qy} X_W Y_{\mathrm{d}W\Psi}, \tag{18c}$$

$$[K_{ij}^{mn}]_{21} = -D_{Qx} X_{\Psi\mathrm{d}W} Y_W, \tag{18d}$$

$$[K_{ij}^{mn}]_{22} = \frac{D_x}{g} X_{\mathrm{d}\Psi} Y_W + \frac{D_{xy}}{2} X_\Psi Y_{\mathrm{d}W} + D_{Qx} X_\Psi Y_W - \omega^2 J_x X_\Psi Y_W, \tag{18e}$$

$$[K_{ij}^{mn}]_{23} = \frac{v_y D_x}{g} X_{\mathrm{d}\Psi W} Y_{W\mathrm{d}\Psi} + \frac{D_{xy}}{2} X_{\Psi\mathrm{d}W} Y_{\mathrm{d}W\Psi}, \tag{18f}$$

$$[K_{ij}^{mn}]_{31} = -D_{Qy} X_W Y_{\Psi\mathrm{d}W}, \tag{18g}$$

$$[K_{ij}^{mn}]_{32} = \frac{v_y D_x}{g} X_{W\mathrm{d}\Psi} Y_{\mathrm{d}\Psi W} + \frac{D_{xy}}{2} X_{\mathrm{d}W\Psi} Y_{\Psi\mathrm{d}W}, \tag{18h}$$

$$[K_{ij}^{mn}]_{33} = \frac{D_y}{g} X_W Y_{\mathrm{d}\Psi} + \frac{D_{xy}}{2} X_{\mathrm{d}W} Y_\Psi + D_{Qy} X_W Y_\Psi - \omega^2 J_y X_W Y_\Psi, \tag{18i}$$

where the following parameters are defined as

$$X_W = \int_0^a W_{xm} W_{xi} \,\mathrm{d}x, \qquad Y_W = \int_0^b W_{yn} W_{yj} \,\mathrm{d}y, \tag{19a}$$

$$X_{\mathrm{d}W} = \int_0^a \frac{\partial W_{xm}}{\partial x} \frac{\partial W_{xi}}{\partial x} \,\mathrm{d}x, \qquad Y_{\mathrm{d}W} = \int_0^b \frac{\partial W_{yn}}{\partial y} \frac{\partial W_{yj}}{\partial y} \mathrm{d}y, \tag{19b}$$

$$X_\Psi = \int_0^a \Psi_{xm} \Psi_{xi} \,\mathrm{d}x, \qquad Y_\Psi = \int_0^b \Psi_{yn} \Psi_{yj} \,\mathrm{d}y, \tag{19c}$$

$$X_{\mathrm{d}\Psi} = \int_0^a \frac{\partial \Psi_{xm}}{\partial x} \frac{\partial \Psi_{xi}}{\partial x} \,\mathrm{d}x, \qquad Y_{\mathrm{d}\Psi} = \int_0^b \frac{\cdot\Psi_{yn}}{\partial y} \frac{\partial \Psi_{yj}}{\partial y} \mathrm{d}y, \tag{19d}$$

$$X_{W\mathrm{d}\Psi} = \int_0^a W_{xm} \frac{\partial \Psi_{xi}}{\partial x} \,\mathrm{d}x, \qquad Y_{W\mathrm{d}\Psi} = \int_0^b W_{yn} \frac{\partial \Psi_{yj}}{\partial y} \mathrm{d}y, \tag{19e}$$

$$X_{\mathrm{d}\Psi W} = \int_0^a \frac{\partial \Psi_{xm}}{\partial x} W_{xi}\,\mathrm{d}x, \qquad Y_{\mathrm{d}\Psi W} = \int_0^b \frac{\partial \Psi_{yn}}{\partial y} W_{yj}\,\mathrm{d}y, \tag{19f}$$

$$X_{\Psi \mathrm{d}W} = \int_0^a \Psi_{xm} \frac{\partial W_{xi}}{\partial x}\,\mathrm{d}x, \qquad Y_{\Psi \mathrm{d}W} = \int_0^b \Psi_{yn} \frac{\partial W_{yj}}{\partial y}\,\mathrm{d}y, \tag{19g}$$

$$X_{\mathrm{d}W\Psi} = \int_0^a \frac{\partial W_{xm}}{\partial x} \Psi_{xi}\,\mathrm{d}x, \qquad Y_{\mathrm{d}W\Psi} = \int_0^b \frac{\partial W_{yn}}{\partial y} \Psi_{yj}\,\mathrm{d}y. \tag{19h}$$

The non-trivial solution of equation (15) is obtained when the determinant $[K]$ equals zero. From the solution, a series ($m = 1, \ldots, M, n = 1, \ldots, N$) of three eigenvalues are extracted; from which the natural frequencies of the plate, denoted as $\omega_{mn}^{(r)}$ ($r = 1, 2, 3$), are computed by taking the square root of these eigenvalues. The lowest frequency is the flexural mode while the two higher frequencies correspond to transverse shear deformations in the $x$ and $y$ directions respectively.

All the sub-matrices of $[K]$ in equation (15) are fully populated and non-zero. Therefore, the solution requires longer computational time. However, certain simplifications can be made without significant loss of accuracy. It can be observed that the elements of the matrix are obtained by integrating the products of beam functions and their derivatives. Consequently, it can be shown that this matrix exhibits a property such that the numerical values of the elements of the sub-matrices on the leading diagonal are much greater than the corresponding elements in the off-diagonal sub-matrices. For this reason, the off-diagonal sub-matrices can be approximated as null sub-matrices. If this is assumed, then equation (15) is simplified as

$$[K_{mn}^{mn}] \begin{Bmatrix} a_{mn} \\ b_{mn} \\ c_{mn} \end{Bmatrix} = 0 \tag{20}$$

and from which the non-trivial solution gives the $(m, n)$ order frequencies $\omega_{mn}^{(r)}$ ($r = 1, 2, 3$). In this manner, significant savings in computational time can be achieved without recourse to a full matrix algorithm.

## 5. FINITE ELEMENT ANALYSIS

A 2-D FE model may be constructed for a flat plate or an equivalent orthotropic plate representing a thin-walled sandwich panel. Similarly, a 3-D FE model may be constructed to analyze a 3-D thin-walled sandwich panel. In this investigation, the *MARC* finite element code [21] was used for both the 2- and 3-D FE study. An eight-node iso-parametric shell element with reduced integration (*element* 22 in *MARC*) was used to idealize the 2-D plate, and for the facing plates and core webs of the 3-D model. One feature of the eight-node iso-parametric element is its ability to account for the effect of transverse shear deformation with two optional patterns;

the transverse shear strain may be assumed constant or as a parabolic distribution across the plate thickness. It should be noted that no shear correction factor is employed in the *MARC* code for the constant distribution pattern. Thus, to compare the present approach with finite element analysis, the shear correction factor in equation (1) should be taken $k^2 = 1{\cdot}0$.

## 6. NUMERICAL EXAMPLES

### 6.1. NATURAL FREQUENCIES OF CLAMPED PLATES

To verify the accuracy of the present approach, the natural frequencies of two clamped homogeneous plates have been computed; an isotropic and an orthotropic plate. Material properties of the plates are provided in reference [18] using the symbols: $D_{11}$, $D_{22}$, $D_{66}$, $D_{12}$, $A_{55}$ and $A_{44}$. These properties are converted to elastic constants shown in this paper, and are listed in Table 1. For the conversion, the following relationships are used to convert the properties:

$$v_x = \frac{D_{12}}{D_{22}}, \qquad v_y = \frac{D_{12}}{D_{11}}, \qquad D_x = D_{11}(1 - v_x v_y), \qquad D_y = D_{22}(1 - v_x v_y), \quad \text{(21a)}$$

$$D_{xy} = 2D_{66}, \qquad D_{Qx} = k^2 A_{55}, \quad D_{Qy} = k^2 A_{44}. \qquad \text{(21b)}$$

Natural frequencies calculated from equation (20), including and excluding the effects of transverse shear, for isotropic plate $A$ are shown in Table 2. To obtain the solution by the present method in which the effect of transverse shear is ignored, the shear stiffnesses $D_{Qx}$ and $D_{Qy}$ was multiplied by a large numerical value. Calculated results are compared with solutions obtained from the Lagrangian multiplier technique [18] including transverse shear, and by the Rayleigh–Ritz method [19] in which shear is neglected; computed numerical values were taken from reference [18]. The present results are in very good agreement with the Lagrangian multiplier

TABLE 1

*Material properties of plates*

| Isotropic plate A | Orthotropic plate B | Moduli of plate B |
|---|---|---|
| $D_x = 0{\cdot}833333 \times 10^3$ lb/in | $D_x = 0{\cdot}196916 \times 10^3$ lb/in | $E_x = 0{\cdot}310002 \times 10^8$ lb/in$^2$ |
| $D_y = 0{\cdot}833333 \times 10^3$ lb/in | $D_y = 0{\cdot}171511 \times 10^2$ lb/in | $E_y = 0{\cdot}270007 \times 10^7$ lb/in$^2$ |
| $D_{xy} = 0{\cdot}62656 \times 10^3$ lb/in | $D_{xy} = 0{\cdot}952820 \times 10^1$ lb/in | $G_{xy} = 0{\cdot}750006 \times 10^6$ lb/in$^2$ |
| $D_{Qx} = 0{\cdot}30921 \times 10^6$ lb/in | $D_{Qx} = 0{\cdot}261555 \times 10^5$ lb/in | $G_{xz} = 0{\cdot}75 \times 10^5$ lb/in$^2$ |
| $D_{Qy} = 0{\cdot}30921 \times 10^6$ lb/in | $D_{Qy} = 0{\cdot}261555 \times 10^5$ lb/in | $G_{yz} = 0{\cdot}75 \times 10^5$ lb/in$^2$ |
| $v_x = 0{\cdot}33$ | $v_x = 0{\cdot}27999$ | |
| $v_y = 0{\cdot}33$ | $v_y = 0{\cdot}024387$ | |
| $\rho = 0{\cdot}1$ lb/in$^3$ | $\rho = 0{\cdot}07412$ lb/in$^3$ | |

TABLE 2

*Natural frequencies* (Hz) *of isotropic plate A*

| Mode $m$ | Mode $n$ | Presetnt solution: Including shear | Presetnt solution: Without shear | Lagrangian multiplier technique* [18] | Rayleigh–Ritz Method [19] |
|---|---|---|---|---|---|
| 1 | 1 | 239·5 | 239·7 | 243·8 | 239·7 |
| 1, 3 | 3, 1 | 877·4 | 879·2 | 891·0 | 879·7 |
| 3 | 3 | 1461·1 | 1465·7 | 1488·3 | 1467·0 |
| 1, 5 | 5, 1 | 2047·8 | 2056·7 | 2088·2 | 2058·9 |
| 3, 5 | 5, 3 | 2605·3 | 2619·1 | 2652·8 | 2622·7 |
| 1, 7 | 7, 1 | 3729·4 | 3756·9 | 3811·7 | 3763·6 |

*$M = N = P = Q = 7$ where $M$ and $N$ are the maximum numbers of modes to be computed, and $P$ and $Q$ are the numbers of multipliers [18].

TABLE 3

*Natural frequencies* (Hz) *of orthotropic plate B*

| Mode $m$ | Mode $n$ | Present solutions: Closed form | Present solutions: Finite element | Lagrangian multiplier technique* [18] |
|---|---|---|---|---|
| 1 | 1 | 129·58 | 129·5 | 127·06 |
| 1 | 2 | 164·69 | 164·6 | 161·48 |
| 1 | 3 | 240·60 | 240·5 | 236·45 |
| 2 | 1 | 340·84 | 340·7 | 334·89 |
| 1 | 4 | 356·64 | 356·4 | 350·52 |
| 2 | 2 | 362·45 | 362·2 | 355·0 |
| 2 | 3 | 412·0 | 411·7 | 405·31 |
| 2 | 4 | 499·50 | 498·9 | 490·91 |

*$M = N = 30$, $P = Q = 15$ where $M$ and $N$ are the maximum numbers of modes to be computed, and $P$ and $Q$ are the numbers of multipliers [18].

and Rayleigh–Ritz solutions. Calculated results, which include the influence of transverse shear, are lower than those without shear, thus correctly reflecting the effects of tranverse shear deformation. By contrast, results from the Lagrangian multiplier technique, which includes the influence of transverse shear, are higher than both the present solution and the Rayleigh–Ritz method.

Calculated closed-form results for orthotropic plate $B$ are shown in Table 3. A 2-D FE analysis was also conducted to obtain the response of the orthotropic plate. The elastic and shear moduli of the plate, which were calculated from equation (1) with $k^2 = 0{\cdot}8225$, are listed in Table 1. In the FE model, 200 elements were used in a $10 \times 20$ mesh. Parabolic transverse shear distribution was incorporated in the FE analysis. The present solutions are in excellent agreement and consistent with the FE result. While all the calculated results are about 0·1% higher than FE results, the Lagrangian multiplier solution is consistently 2% lower than FE results. It should be noted that in the Lagrangian multiplier technique, the number of Lagrangian multipliers ($P$ or $Q$) should be equal to the maximum number of modes ($M$ or $N$) for the boundary conditions to be satisfied. Otherwise, the displacements obtained by this technique may not satisfy completely the clamped boundary condition. This explains the lower frequencies compared with FE results. This example demonstrates the validity of the present approach.

### 6.2. NATURAL FREQUENCY OF TRUSS-CORE SANDWICH PANEL

Since the accuracy of the present approach has been demonstrated, attention can be focused on determining the vibration characteristics of a thin-walled truss-core sandwich panel as an equivalent homogeneous orthotropic thick plate. For this example, consider an aluminum sandwich panel of length $a = 2$ m ($x$ direction) and width $b = 1{\cdot}2$ m ($y$ direction). The panel width implies an assembly of eight identical truss-core sandwich units. Dimensions and properties of the unit are: $p = 75$ mm, $f_0 = 25$ mm, $d = 46{\cdot}75$ mm, $t_f = t_c = 3{\cdot}25$ mm, $E = 80$ GPa, the Poisson ratio $\nu = 0{\cdot}3$, and material density $\rho = 2700\ \text{kg/m}^3$.

Using equation (2), the truss-core sandwich panel is transformed into a homogeneous orthotropic thick plate. The seven calculated elastic constants for the thick plate continuum are shown in Table 4 (column 2). Note the relatively low shear stiffness $D_{Qy}$ compared with $D_{Qx}$ of the panel. Equivalent material properties of the orthotropic thick plate calculated from equation (1) are also listed in the table for two cases: $k^2 = 0{\cdot}8225$ and $k^2 = 1$. The latter value indicates no transverse shear correction made to the shear stiffness moduli $G_{xz}$ and $G_{yz}$.

Free vibration analysis was undertaken for the clamped orthotropic thick plate using the derived closed-form solution and FE methods. In the 2-D FE model with the assumption of parabolic shear distribution, appropriate equivalent material properties in Table 4 are used. For constant shear distribution, no transverse shear correction is necessary. Hence, parameters from the last column of Table 4 are used in the 2-D FE analysis. A 3-D FE model of the truss-core panel was constructed and analyzed to obtain the response. In this case, original material properties as detailed in the first column of Table 4 are used.

The 2-D FE model for the plate is a $10 \times 20$ mesh comprising 200 elements. Since the shear stiffness of the panel is considerably weaker in the $y$ direction, the mesh was made denser in this direction. To confirm convergence, a parallel study was conducted in which the mesh was refined by a factor of two in both directions, resulting in a 2-D model consisting of 800 elements. The generated 3-D FE mesh is shown in Figure 4. For this model, 960 elements were used.

TABLE 4

*Elastic constants and equivalent material properties of truss-core panel*

| Material properties | Elastic constants and equivalent density | Equivalent material properties | |
|---|---|---|---|
| | | $k^2 = 0{\cdot}8225$ | $k^2 = 1$ |
| $E = 80$ GPa | $D_x = 0{\cdot}3111 \times 10^3$ kN/m | $E_x = 36\,536$ MPa | $E_x = 36\,536$ MPa |
| $\nu = 0{\cdot}3$ | $D_y = 0{\cdot}2864 \times 10^3$ kN/m | $E_y = 33\,631$ MPa | $E_y = 33\,631$ MPa |
| $\rho = 2700$ kg/m$^3$ | $D_{xy} = 0{\cdot}2186 \times 10^3$ kN/m | $G_{xy} = 12\,834$ MPa | $G_{zy} = 12\,834$ MPa |
| | $D_{Qx} = 53722$ kN/m | $G_{xz} = 1397$ MPa | $G_{xz} = 1149{\cdot}1$ MPa |
| | $D_{Qy} = 913$ kN/m | $G_{yz} = 23{\cdot}76$ MPa | $G_{yz} = 19{\cdot}54$ MPa |
| | $\nu_x = 0{\cdot}3$ | $\nu_{xy} = 0{\cdot}3$ | $\nu_{xy} = 0{\cdot}3$ |
| | $\nu_y = 0{\cdot}2761$ | $\nu_{yx} = 0{\cdot}2761$ | $\nu_{yx} = 0{\cdot}2761$ |
| | $\rho_e = 498{\cdot}86$ kg/m$^3$ | $\rho_e = 498{\cdot}86$ kg/m$^3$ | $\rho_e = 498{\cdot}86$ kg/m$^3$ |
| For 3-D FE model | For closed-form solution | For 2-D FE model with parabolic shear | For 2-D FE model with constant shear |

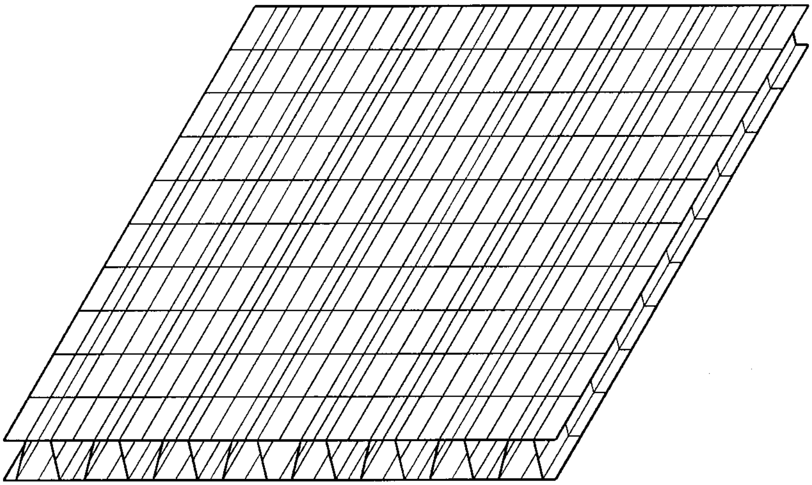

Figure 4. 3-D FE model of truss-core sandwich panel (960 elements).

Computed responses from FE methods (with constant and parabolic shear strain distribution across the plate thickness) and from closed-form solution are summarized in Table 5. Only the first 10 vibration modes are shown and all are associated with flexural deformation of the panel. The results may be summarized as follows:

- Calculated closed-form solutions are in very good agreement with 2- and 3-D finite element output regardless of the influence of transverse shear. Detailed

TABLE 5

*Natural frequencies* (Hz) *of truss-core sandwich panel*

| Vibration mode | $m$ | $n$ | 3-D FE 960 elements $\gamma_0$ | 3-D FE 960 elements $\gamma_2$ | 2-D FE 200 elements $\gamma_0$ | 2-D FE 200 elements $\gamma_2$ | 2-D FE 800 elements $\gamma_0$ | 2-D FE 800 elements $\gamma_2$ | Closed form solution |
|---|---|---|---|---|---|---|---|---|---|
| 1 | 1 | 1 | 139·3 | 139·3 | 138·7 | 138·6 | 138·7 | 138·7 | 138·8 |
| 2 | 1 | 2 | 213·6 | 213·4 | 210·9 | 210·7 | 211·1 | 210·9 | 211·4 |
| 3 | 1 | 3 | 297·4 | 297·1 | 293·7 | 293·4 | 294·2 | 293·9 | 294·6 |
| 4 | 2 | 1 | 290·0 | 290·0 | 294·3 | 294·3 | 294·8 | 294·7 | 294·9 |
| 5 | 1 | 4 | 348·1 | 348·0 | 351·2 | 351·1 | 352·1 | 351·9 | 352·9 |
| 6 | 2 | 2 | 382·0 | 381·6 | 377·8 | 377·5 | 378·9 | 378·5 | 379·6 |
| 7 | 1 | 5 | 426·2 | 426·0 | 429·6 | 429·4 | 431·2 | 430·9 | 432·5 |
| 8 | 1 | 6 | 466·2 | 465·6 | 461·3 | 460·8 | 463·2 | 462·7 | 464·2 |
| 9 | 2 | 3 | 501·6 | 501·5 | 515·1 | 514·7 | 517·7 | 517·4 | 519·8 |
| 10 | 1 | 7 | 509·5 | 509·1 | 519·1 | 518·9 | 521·3 | 521·2 | 521·4 |

$\gamma_0$ Constant distribution of transverse shear strain across the thickness.
$\gamma_2$ Parabolic distribution of transverse shear strain across the thickness.

comparison of the closed-form solution with the 2-D model indicates an error less than 1% for all frequencies. With the 3-D model, the largest error was about 3·6%. This occurs in the ninth mode of the 3-D model incorporating a parabolic transverse shear distribution. In the majority of cases, the error was less than 0·5% for the 2-D model and 1·0% for 3-D model. This comparison demonstrates the validity and synergy of the transformation process from a 3-D thin-walled truss-core sandwich structure to a 2-D orthotropic thick plate continuum, as well as the accuracy of the closed-form approach.

- Refining the mesh of the 2-D model does not significantly increase the accuracy of the results. The 2-D model with 200 elements was considered sufficiently accurate for analysis.

## 7. CONCLUSIONS

The truss-core sandwich panel and its potential benefits have been introduced, and elastic constants have been provided to enable the transformation of a 3-D structure into an equivalent homogeneous orthotropic thick plate continuum. A closed-form solution for the dynamic analysis of clamped orthotropic thick plate has been presented. Calculated dynamic response using the closed-form solution, which includes the influence of transverse shear, is compared with the Lagrangian multiplier and finite element methods. The comparison is a clear indication of the accuracy of the closed-form solution. Following this validation exercise, the closed-form technique was extended to a truss-core sandwich panel. The dynamic response of the equivalent orthotropic thick plate was computed and the results were compared with 2- and 3-D FE analyses since no analytical solution exists. In the finite element analyses, the influence of transverse shear deformation was included with parabolic or constant distribution across the plate thickness. The good agreement further amplifies the synergy of the transformation process and accuracy of derived elastic constants and closed-form solution. This synergy provides significant savings in computational effort and in the modelling process of clamped truss-core sandwich panels. The derived closed-form solution can be used for bending and dynamic response analysis of clamped orthotropic plates and sandwich panels.

## 8. SUMMARY

In the absence of an analytical solution for the dynamic response of thin-walled sandwich panels, the 3-D finite element (FE) method is commonly used to determine behavior. However, this method may not find favor amongst practitioners if they are unfamiliar with both hardware and software. An alternative to 3-D FE method is to transform the sandwich structure into an equivalent homogenous orthotropic thick plate continuum, for which a closed-form solution and 2-D FE methods may be used to evaluate the response. This paper presents derived expressions of elastic constants including the effects of transverse shear, thereby allowing a truss-core sandwich panel to be analyzed as an equivalent orthotropic thick plate. The truss-core sandwich panel is characterized by an extrusion unit, which differs in many respects from the fabrication process of conventional sandwich panels, but the principle of a core, sandwiched between and separating two facing sheets is retained. The advantages of the truss-core unit are outlined. Using the derived equivalent elastic constants in conjunction with a closed-form solution, the free vibration response of a clamped truss-core sandwich panel as a homogenous orthotropic thick plate continuum is presented. A double series solution is used for the clamped orthotropic thick plate. Numerical examples, including the influence of transverse shear on the response, show that the closed-form solution agrees well with both 3- and 2-D finite element results. Thus, the effectiveness of the synergistic transformation process and the accuracy of the dynamic closed-form solution are proved.

## REFERENCES

1. F. J. Plantema 1966 *Sandwich Construction: The Bending and Buckling of Sandwich Beams, Plates and Shells*. New York: Wiley.
2. H. G. Allen 1969 *Analysis and Design of Structural Sandwich Panels*. Oxford: Pergamon Press.
3. C. Libove and R. H. Hubka 1951 *National Aeronautics and Space Administration (NASA) Technical Note* 2289. Elastic constants for corrugated core sandwich plates.
4. P. Montague and C. Norris 1987 *Proceedings of the International Conference on Steel and Aluminium Structures* (Cardiff, UK), (R. Narayanan editor), 564–574, Elsevier Amsterdam. Spot-welded, corrugated-core, sandwich steel panels subjected to lateral load.

5. C. Norris, P. Montague and K. H. Tan 1989 *The Structural Engineer* (London) **67**, 167–176. All-steel sandwich panels to carry lateral load: experimental and theoretical behaviour.
6. K. H. Tan, P. Montague and C. Norris 1989 *The Structural Engineer* (London) **67**, 159–166. Steel sandwich panels: finite element, closed solution, and experimental comparison, on a 6 m × 2.1 m panel.
7. T. C. Fung, K. H. Tan and T. S. Lok 1993 *Proceedings of the third International Offshore and Polar Engineering Confer*. (CO, USA), Vol. **4**, 244–249. Analysis of C-core sandwich plate decking.
8. T. C. Fung, K. H. Tan and T. S. Lok 1994 *ASCE Journal of Structural Engineering* **120**, 3046–3065. Elastic constants for *Z*-core sandwich panels.
9. T. S. Lok and Q. H. Cheng 1999 *Proceedings of the Ninth International Offshore and Polar Engineering Conference and Exhibition*, (Brest, France), Vol. 4, 292–298. Equivalent stiffness parameters of truss-core sandwich panel.
10. K. H. Tan, T. C. Fung and T. S. Lok 1993 *The Structural Engineer* (London) **71**, 253–258. A simplified thick plate analogy for the analysis of all-steel sandwich panels.
11. T. S. Lok and Q. H. Cheng 1999 *Proceedings of the Seventh East Asia-Pacific Conference on Structural Engineering and Construction* (*Kochi*, *Japan*), 285–290. Closed-form solution for the free vibration of a truss-core sandwich panel.
12. A. W. Leissa 1969 *Vibration of Plates*. National Aeronautics and Space Administration.
13. T. Sakata and K. Hosokawa 1988 *Journal of Sound and Vibration* **125**, 429–439. Vibrations of clamped orthotropic rectangular plates.
14. D. J. Gorman 1990 *Journal of Sound and Vibration* **140**, 391–341. Accurate free vibration analysis of clamped orthotropic plates by the method of superposition.
15. N. Li 1992 *Journal of Sound and Vibration* **158**, 307–316. Forced vibration analysis of the clamped orthotropic rectangular plate by the superposition method.
16. M. Dalaei and A. D. Kerr 1966 *Journal of Sound and Vibration* **189**, 399–406. Natural vibration analysis of clamped rectangular orthotropic plates.
17. A. N. Bercin 1996 *Journal of Sound and Vibration* **196**, 243–247. Free vibration solution for clamped orthotropic plates using the Kantorovichi method.
18. R. L. Ramkumar, P. C. Chen and W. J. Sanders 1987 *American Institute of Aeronautics and Astronautics Journal* **25**, 146–151. Free vibration solution for clamped orthotropic plates using Lagrangian multiplier technique.
19. J. E. Ashon and J. M. Whitney 1970 *Theory of Laminated Plates*. Stamford, CT: Technomic.
20. C. Libove and S. B. Batdorf 1948 *National Advisory Committee for Aeronautics* (*NACA*) *Technical Note* 1526. A general small-deflection theory for flat sandwich plates.
21. MARC Analysis Research Corporation 1994 *MARC K*6·0 *documents Vol. B-Element Library*.